Dalton Transactions

An international journal of inorganic chemistry

www.rsc.org/dalton

Volume 41 | Number 47 | 21 December 2012 | Pages 14213–14440

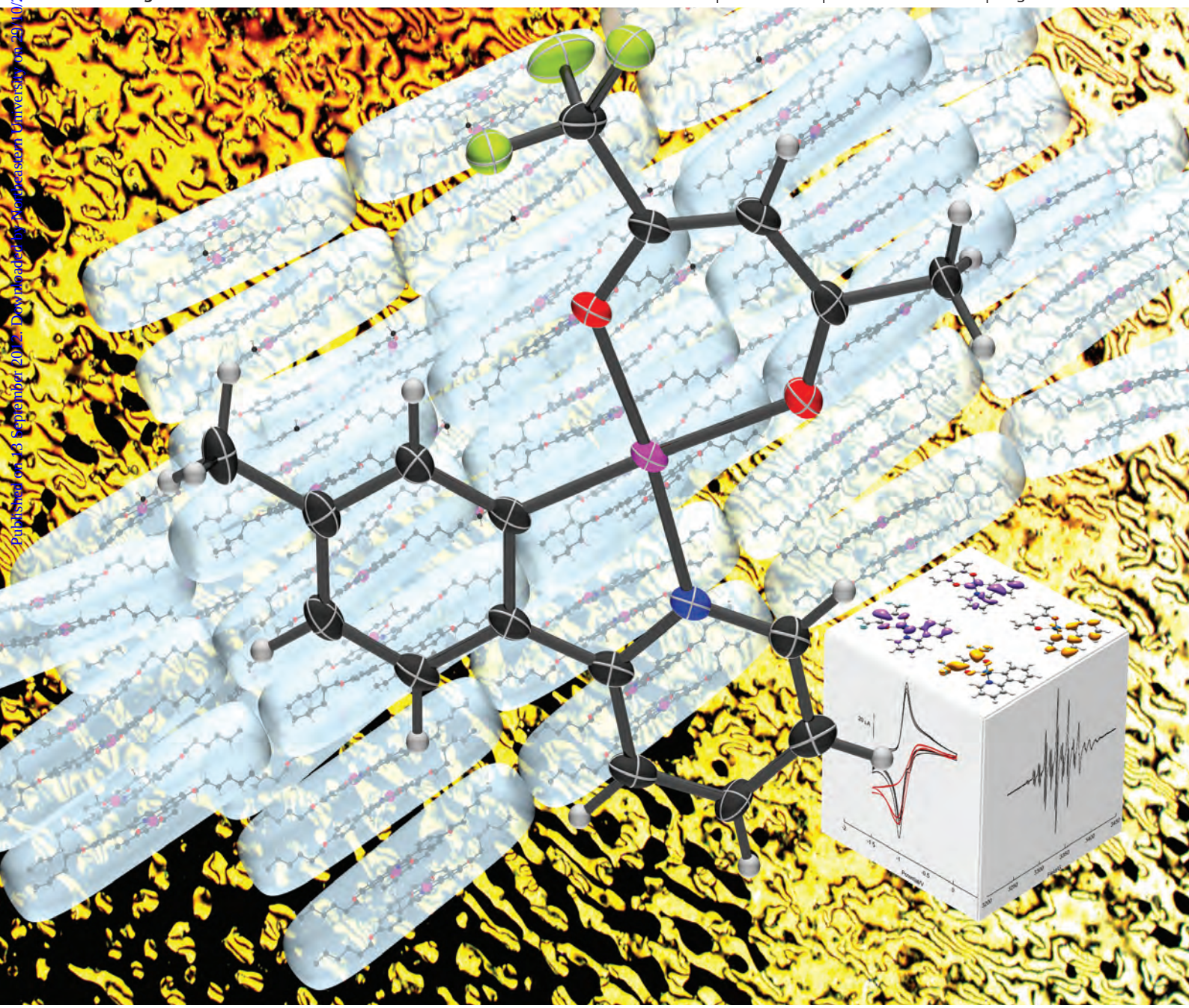

ISSN 1477-9226

RSC Publishing

COVER ARTICLE

Bruce *et al.*

Phosphorescent, liquid-crystalline complexes of platinum(II): influence of the β-diketonate co-ligand on mesomorphism and emission properties

1477-9226(2012)41:47;1-H

Dalton Transactions

Cite this: *Dalton Trans.*, 2012, **41**, 14244

www.rsc.org/dalton

PAPER

Phosphorescent, liquid-crystalline complexes of platinum(II): influence of the β-diketonate co-ligand on mesomorphism and emission properties†‡

Matthew Spencer,[a] Amedeo Santoro,[a] Gemma R. Freeman,[b] Álvaro Díez,[a] Paul R. Murray,[c] Javier Torroba,[a] Adrian C. Whitwood,[a] Lesley J. Yellowlees,[c] J. A. Gareth Williams[b] and Duncan W. Bruce*[a]

Received 11th July 2012, Accepted 30th August 2012
DOI: 10.1039/c2dt31525d

Two series of rod-like *ortho*-platinated complexes bound to a range of β-diketonate co-ligands are reported of the form [Pt(*N^C*)(*O^O*)]. The liquid crystal and luminescent properties are influenced through the introduction of different β-diketonates (*O^O*) as well as through the presence of a fused cyclopentene ring on the *N^C*-coordinated 2-phenylpyridine ligand. For metal complexes, smectic phases are dominant but no mesomorphism is exhibited when the β-diketonate is hexafluorinated acetylacetonate (1,1,1-5,5,5-hexafluoro-2,4-pentandione). The introduction of an unsymmetrical trifluoroacetyl acetonate (1,1,1-trifluoro-2,4-pentandione) ligand is particularly interesting due to the discovery of the β-diketonate as a dynamic system that readily isomerises to a 1 : 1 ratio under thermal conditions, from an initial ratio of 3 : 1 formed during the synthesis. As expected, the presence of the 3,5-heptanedionato co-ligand decreases the transition temperatures due to the introduction of a larger lateral substituent. Unfortunately complexes based on 2-phenylpyridine ligands with a fused cyclopentene ring are, with one exception, not mesomorphic. With the exception of the hexafluoroacetyl acetonate complexes, the materials are brightly luminescent and have excited state lifetimes between 13 and 30 μs with emission quantum efficiencies exceeding 0.5, with one as high as 0.7. A time-dependent density functional theory (TD-DFT) study suggests that the lack of emission from the hexafluoroacetyl acetonate complexes may be associated with large structural distortion upon formation of the excited state, as well as to poorer overlap of orbitals leading to a lower radiative rate constant. The same analysis provides an explanation for the apparently quite different emission efficiencies of the two isomers of the trifluoroacetyl acetonate complexes.

Introduction

There are several different devices where luminescence or charge transport is one of the key points for development required for profitable application in the marketplace. Indeed, in the last ten years, significant effort has been invested in research into new materials for, *inter alia*, organic light emitting diodes (OLEDs), thin-film transistors (TFT devices), organic solar cells, new photo-active materials, bio-active molecules, charge-transport devices, active components for imaging and data treatment.[1] The cooperativity of physical properties could improve the efficiency of these devices greatly and it is in this environment that our research is mainly focused. For example, it has been reported that liquid-crystal order, and an organised supramolecular structure in general, is expected to improve charge mobility,[2] while Sagara and Kato,[3] and Kozhevnikov *et al.*[4] have independently demonstrated in recent studies that liquid-crystal order can influence the emission of materials under mechanical stimuli, thermal phase transitions or both. From this point of view and in particular because of the greater efficiency of emission from many metals complexes that can access the triplet manifold, phosphorescent, metal-containing liquid crystals represent an interesting target and challenge.[5]

Square planar *ortho*-metallated platinum complexes are a group of molecules that have been studied widely in several different research fields.[6,7] These complexes have proved popular in part because their chemical and physical properties can be tuned by systematic change or modification of the ligands around the metal centre. In particular, the fact that the HOMO and LUMO tend to be localised on different parts of the molecule allows their energies to be controlled relatively independently.[8] Although numerous examples of brightly emissive platinum-containing materials have emerged over recent years,[6,7] only a few reports describe a combination of liquid crystal and luminescent properties.[3,5c,9] In this context, we recently reported very efficient luminescent phenylpyridine platinum complexes bearing acetylacetonate as the co-ligand [Pt(*N^C*)(acac)],[9d] with

[a]*Department of Chemistry, University of York, Heslington, York YO10 5DD, UK. E-mail: duncan.bruce@york.ac.uk; Tel: +44 (0)1904 324085*
[b]*Department of Chemistry, University of Durham, University Science Laboratories, South Road, Durham, DH1 3LE, UK*
[c]*School of Chemistry, Joseph Black Building, University of Edinburgh, West Mains Road, Edinburgh, EH9 3JJ, UK*

†Dedicated to Professor David Cole-Hamilton on the occasion of his retirement and to recognise his outstanding contributions to chemistry.
‡Electronic supplementary information (ESI) available. CCDC 885300 and 884157. For ESI and crystallographic data in CIF or other electronic format see DOI: 10.1039/c2dt31525d

emission quantum efficiencies > 0.5, the highest yet reported for a ppy derivative of platinum; the materials were also liquid crystals. As part of this study, we also demonstrated the influence of a cyclopentane ring fused onto the pyridine ring on the luminescence and liquid crystallinity.

We have now extended this investigation into the influence of the *O^O*-coordinated β-diketonate co-ligand on liquid crystal and luminescent properties. Specifically, we have examined hexafluoroacetylacetonate (hfac), trifluoroacetylacetonate (tfac) and heptanedionate (hdn) in place of the acetylacetonate (acac) ligand of the previous studies. Two series of cyclometallated platinum complexes have been synthesised, with and without cyclopentane rings fused to the pyridyl ring, bearing these three different *O^O*-diketonate ligands groups. The synthesis, liquid crystal and luminescence properties of these new compounds are described here, together with the crystal structure of two of the compounds and an EPR study used to rationalise the behaviour of the hexafluorinated complexes. Density functional theory (DFT) and time-dependent DFT (TD-DFT) are used to shed light on the significant effect of the *O^O* co-ligand on the ground and excited state properties of the complexes.

Results and discussion

Synthesis

The complexes were prepared according to the scheme shown as Scheme 1, which follows exactly the methodology reported earlier.[9d] Thus, the ligands (**1**) were prepared from 1,2,4-triazine precursors using an inverse electron demand Diels–Alder protocol and were then reacted with $K_2[PtCl_4]$ in HOAc to give the rather insoluble di-μ-chloro dimer (**2**). Heating the dimers in dmso led to the intermediate complexes with coordinated dmso (**3**), which were very soluble and gave good conversion to the target complexes (**4 to 11**) when reacted with the sodium salts of the β-diketone. It is noted in passing that attempts to prepare the complex containing bound dmso directly from the ligand and *cis*-$[PtCl_2(S\text{-dmso})_2]$ resulted in oxidation to Pt^{III} when carried out in HOAc.[10] The range of complexes synthesised is shown in Scheme 1.

Crystal and molecular structure of complex 5–6

In the case of **5**–6, it was possible to obtain crystals suitable for a single crystal diffraction study, the results of which are now described.

Thus, the complex crystallised in the monoclinic space group $P2_1/n$ with two complexes in the asymmetric unit (Fig. S1‡). There was evidence of twinning in the crystal which led to significant residual peaks in the difference map. These were close to C9, C33, C45 and C69 and were believed to correspond to the sites of the platinum atoms in the twins. Identical twinning was observed for a data set from a different crystal, which means that the twinning is a systematic process inherent in formation of the crystals. The twinning caused the ADP of C9, C33, C45 and C69 to be distorted and so these atoms were restrained to be approximately isotropic. One of the methyl groups of the acac (C66) was disordered and modelled in two positions with a refined occupancy of 66 : 34. Key data are found in Table 1, while the molecular structure of the one of the complexes from the asymmetric unit (prepared using a cif file with the disorder removed) is shown as Fig. 1.

Comparison of the four bond lengths to Pt (Table 2) shows that, within the confidence level of the ESDs, there are no differences between the two complexes in the asymmetric unit and, while it is a close-run thing in one case, there is also no statistically significant difference between any of the Pt–N and Pt–C distances. However, this does not extend to the Pt–O bond lengths where in each case, the bond length *trans* to the Pt–C bond is longer, as expected on the basis of *trans*-influence. Analysis of intermolecular contacts at the level of sum of the van der Waals' radii minus 0.1 Å shows none that could be regarded as structure directing.

Liquid crystal properties of the ligands and complexes

The detail of the mesomorphic behaviour of the ligands was reported earlier.[9d] Thus, ligands without the fused five-membered ring showed a variety of smectic phases with clearing points up to almost 240 °C, while when the five-membered ring was present, only a nematic phase was seen with all clearing points lower than 115 °C. Such a change in behaviour is entirely consistent with the introduction of a bulky, lateral substituent. In terms of the complexes, binding of Pt and acac simplified the mesomorphism a great deal so that only SmA phases were observed.

In the current work, use of the heptanedionato co-ligand with the unsubstituted phenylpyridine ligands also gave complexes that showed a SmA phase, but the extra flexibility of the lateral ligand affected the transition temperatures (Table 3). Thus, melting points were typically suppressed by around 50 °C, while clearing points dropped by about 25 °C. For example, with acac, the C10 homologues showed Cr ·168 · SmA · 244 · Iso, while with hdn the transitions were Cr · 116 · SmA · 217 · Iso. The greater drop in the melting point meant that the liquid crystal range also increased (76 to 101 °C in this example).

However, the situation for the tfac co-ligands was more complicated owing to the presence of isomers (Fig. 2). Previously, we had studied *ortho*-metallated benzylidene aniline complexes of Pd and Pt with a tfac co-ligand and had come across the same issue of isomers, but in each case, the synthesis led to a 1 : 1 mixture which behaved as a single material implying, coincidentally, that the 1 : 1 mixture was almost eutectic in nature.[11] However, with the present materials, the situation was somewhat different.

Thus, it was found that simple synthesis of the complexes led to a 3 : 1 mixture of two isomers, represented in Fig. 2, as evidenced by the appearance in the ^1H NMR spectrum of two singlets at δ = 5.80 (intensity 3) and 5.84 (intensity 1) from the γ (methine) hydrogen. When the mixtures were heated, the C8, C10 and C12 homologues showed a SmA phase, while the C6 material showed a nematic phase. However, what was interesting was that it was clear that the two isomers interconverted in the melt so that after some time in the mesophase the ratio of the two was 1 : 1. This was investigated in a little more detail for complex **6**–8, which melted totally to the SmA phase at 147 °C. Thus, a dry sample (3 : 1 ratio of isomers) was heated at various

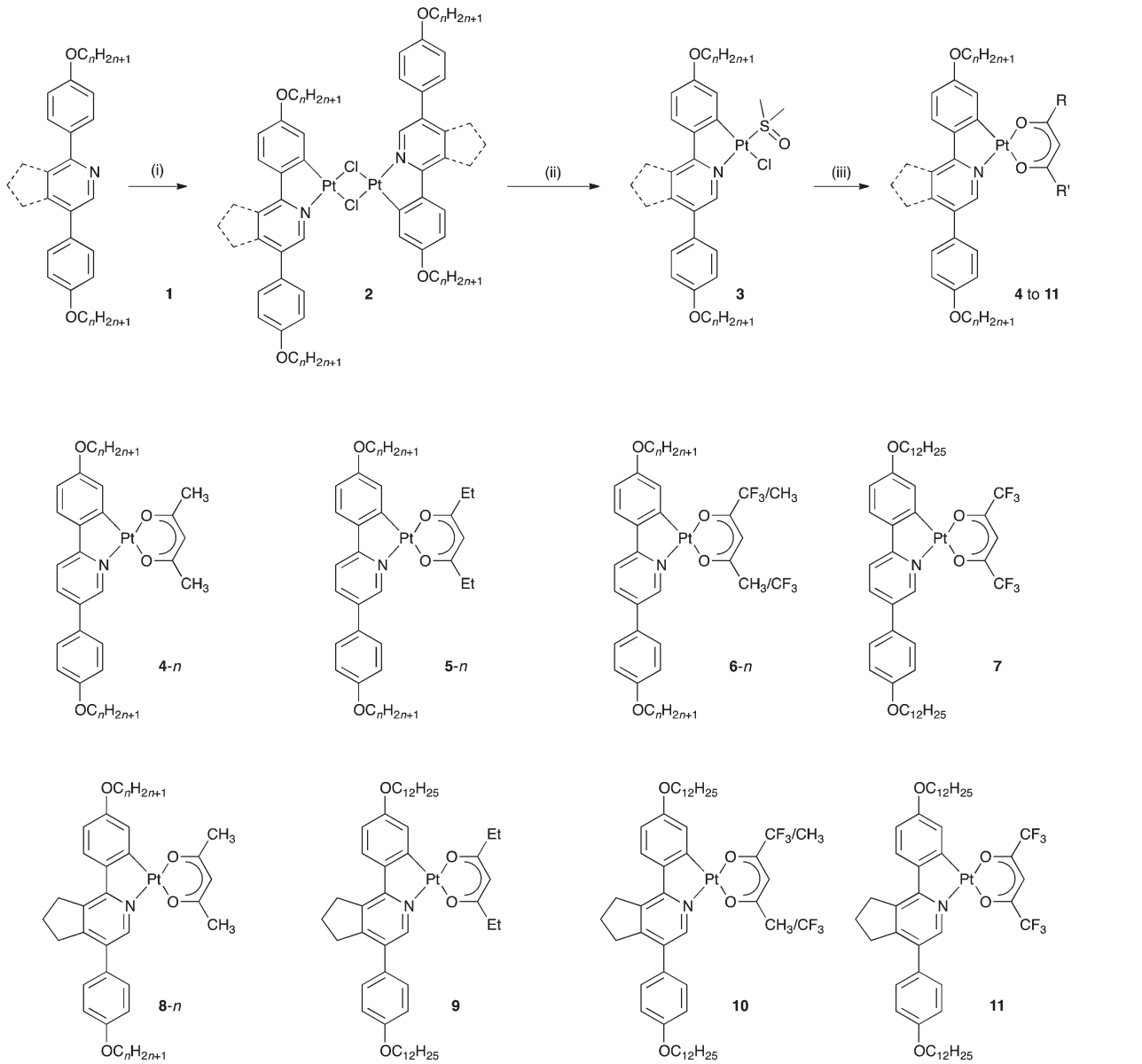

Scheme 1 Preparation of the platinum β-diketonate complexes (*n* refers to the number of carbons in the alkoxy chain) of diphenylpyridine ligands and structures of complexes prepared (**4**-*n* and **8**-*n* were prepared and reported previously[9d]). Conditions: (i) $K_2[PtCl_4]$/HOAc/reflux/24 h; (ii) dmso/reflux/30 min; (iii) Na^+(β-diketonate)$^-$/CH_2Cl_2/rt/8 h. Procedures are the same for ligands/complexes with or without fused C_5 ring. The structures of **6**-*n* and of **10** imply the two different isomers of the coordinated tfac ligand.

temperatures for an hour after which the ^{1}H NMR spectrum was recorded. The spectra revealed that up to 140 °C there was no isomerism, while at 160 °C the ratio changed to 1.3 : 1, while at 170 °C it reached 1 : 1. More rapid isomerisation could be achieved by intermittent heating of small amounts of the solid with a heat gun.

However, despite this isomerisation, each component underwent phase changes independently so that it was clear that a eutectic was not formed and the two forms appeared immiscible, leading to the appearance of two, co-existing states (*e.g.* Cr and N or N and Iso) at some temperatures. Thus, the data in Table 2 are for 1 : 1 mixtures that have been isomerised thermally. The isomerism will be discussed in greater detail below, but it is important to note the changes in transition temperature that resulted from the use of tfac. Thus, the most significant observation was the destabilisation of both the crystal and mesophase. The crystal phase was destabilised by between 30 and 80 °C, while the clearing points were destabilised by up to 90 °C. Of course, these temperatures are those of 1 : 1 mixtures and so there will be a destabilisation associated simply with the fact that, as far as melting and clearing points are concerned, the complexes can be regarded as 'impure'. However, previous studies comparing mesomorphism of acac and tfac complexes of Pd^{II} complexes showed destabilisation of clearing points by around 60 °C and in this and these previous cases, it is the greater size of CF_3 compared to CH_3 that is held responsible.[11]

In the complex incorporating hfac as the *O^O* co-ligand, it was found that all mesomorphism was suppressed and the

Table 1 Crystallographic parameters for complexes **5**–6 and **12**

	5–6	**12**
CCDC code	885300	884157
Empirical formula	$C_{36}H_{47}NO_4Pt$	$C_{17}H_{14}F_3NO_2Pt{\cdot}(CHCl_3)_{0.5}$
Formula weight/g mol^{-1}	752.84	576.07
T/K	110(2)	110.00(10)
Crystal system	Monoclinic	Triclinic
Space group	$P2_1/n$	$P\bar{1}$
a/Å	13.1603(11)	11.988(2)
b/Å	12.8623(11)	12.8040(14)
c/Å	38.458(3)	13.095(2)
α/°	90	86.305(12)
β/°	93.993(2)	69.598(16)
γ/°	90	77.406(12)
V/Å^3	6494.0(9)	1838.5(5)
Z	8	4
ρ_{calc}/Mg m^{-3}	1.540	2.081
F(000)	3040	1092
Crystal size/mm^3	0.26 × 0.16 × 0.04	0.1581 × 0.1275 × 0.0673
θ range for data collection/°	1.60 to 25.04	5.64 to 64.36°
Index ranges	$-15 \le h \le 15$, $-15 \le k \le 15$, $-45 \le l \le 45$	$-13 \le h \le 17$, $-19 \le k \le 18$, $-17 \le l \le 19$
Reflections collected	49 929	17 553
Independent reflections	11 460 [R_{int} = 0.0446]	11 514[$R_{(int)}$ = 0.0264]
Data/restraints/parameters	11 460/32/785	11 514/18/481
Goodness-of-fit on F^2	1.115	1.029
Final R indices [$I > 2\sigma(I)$]	R_1 = 0.0418, wR_2 = 0.0907	R_1 = 0.0459, wR_2 = 0.1031
R indices [all data]	R_1 = 0.0524, wR_2 = 0.0947	R_1 = 0.0622, wR_2 = 0.1141
Largest diff. peak/hole/e Å^{-3}	2.95 and −3.04	11.81/−1.83

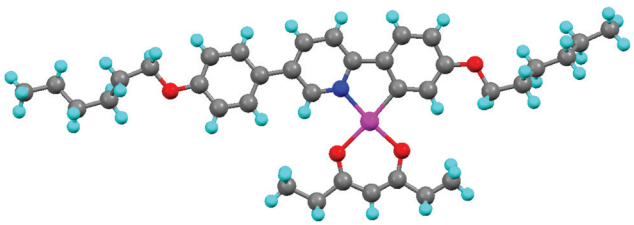

Fig. 1 Molecular structure of one of the complexes present in the asymmetric unit of complex **5**–6. An ORTEP representation is found as Fig. S1(b).‡

Table 2 Pt-ligand bond lengths in complexes **5**–6 and **12**

	5–6 (complex 1)	**5**–6 (complex 2)	**12** (complex 1)	**12** (complex 2)
d_{Pt-C}/Å	1.973(7)	1.968(7)	1.966(6)	1.965(6)
d_{Pt-N}/Å	1.991(5)	2.001(5)	1.997(6)	1.990(5)
$d_{Pt-O(trans\ to\ C)}$/Å	2.089(4)	2.082(5)	2.083(5)	2.093(4)
$d_{Pt-O(trans\ to\ N)}$/Å	2.009(4)	1.994(4)	2.017(5)	1.996(5)

complex simply melted to an isotropic fluid at 151 °C. Precedent suggests that the reduction in anisotropy consequent on the introduction of two CF_3 groups accounts for this large mesophase destabilisation.[11]

The complexes of the ligand with the fused five-membered ring were then studied, but it was little surprise that, with two increments of lateral broadening, neither the complex with tfac nor hfac was mesomorphic and that with heptanedionate showed only a monotropic SmA phase at 87 °C. These complexes were therefore not studied further.

Isomerisation in the tfac complexes

The possibility that the two isomers of the tfac complexes might have different photophysical properties from one another (*vide infra*) prompted us to investigate whether the isomers could be separated, despite their lability in the melt. First, attempts were made selectively to prepare one isomer by changing either solvent or temperature, the results of which are collected in Table 4.

Evidently one isomer can be favoured over the other, but even from these preliminary experiments it seemed evident that regioselective synthesis was unlikely. Then, given that isomerisation was possible in the melt, the analogous process was investigated in solution, so that a 3 : 1 mixture of isomers was heated under reflux for one hour in CH_2Cl_2, $CHCl_3$ and CH_3CN, but within experimental error, no change in ratio could be observed.

More success in isolating a single isomer was obtained by fractional crystallisation from acetone, where the less soluble isomer (that with the methine hydrogen at δ = 5.80) could be concentrated, after three successive crystallisations, to 36 : 1 (based on the ^{1}H NMR integration). With this isomer in hand, exhaustive attempts were made to grow single crystals in order to characterise the isomer obtained, but none was successful. Similarly, none of the NOE experiments carried out was able to provide any evidence as to the identity of the isomer present.

Molecular structure of the single isomer of a tfac complex of Pt-2-(4-tolyl)pyridine

Frustrated by the failure of these attempts to allow characterisation of the isomer, a different strategy was employed in which a simpler complex, incorporating 2-tolylpyridine as the *N^C* ligand, was prepared. Fractional crystallisation of this complex

Table 3 Thermal behavior of complexes from **4**-*n* to **11**

Compound[a]	Transition	*T*/°C	Compound	Transition	*T*/°C
4–6	Cr–SmA	200	**6**–6[b]	Cr–Cr + N	134
	SmA–Iso	237.5		Cr + N–N	143
4–8	Cr–SmA	190		N–N + Iso	145
	SmA–dec	250		N + Iso–Iso	150
4–10	Cr–SmA	168	**6**–8[b]	Cr–Cr + SmA	135
	SmA–Iso	244		Cr + SmA–SmA	147
4–12	Cr–SmA	170		SmA–SmA + Iso	149
	SmA–I	231		SmA + Iso–Iso	166
5–6	Cr–SmA	169	**6**–10[b]	Cr–SmA	133
	SmA–Iso	228		SmA–SmA + Iso	144
5–8	Cr–SmA	148		SmA + Iso–Iso	158
	SmA–I	225	**6**–12[b]	Cr–Cr + SmA	90
5–10	Cr–SmA	116		Cr + SmA–SmA	114
	SmA–Iso	217		SmA–SmA + Iso	128
5–12	Cr–SmA	100		SmA + Iso–Iso	164
	SmA–Iso	205	**9**	Cr–Iso	108
7	Cr–Iso	151		(SmA–Iso)	(87)
8–6	Cr–Iso	161	**10**[b]	Cr–Cr + Iso	105
	(N–Iso)	(101)		Cr + Iso–Iso	115
8–8	Cr–Iso	141	**11**	Cr–Iso	126
	(SmA–N)	(110)			
	(N–Iso)	(115)			
8–10	Cr–Iso	123			
	(SmA–Iso)	(115)			
8–12	Cr–Iso	121			
	(SmA–Iso)	(119)			

[a] Data for complexes **4**-*n* and **8**-*n* from ref. 9*d*. [b] Behaviour is of a pre-equilibrated 1 : 1 isomer mixture (see text).

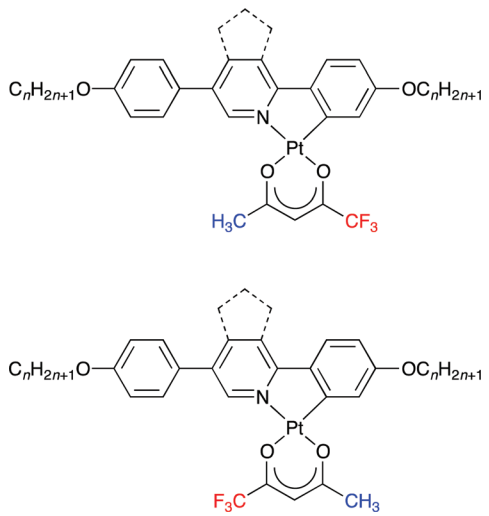

Fig. 2 The tfac complexes **6**-*n* and **10** were found to comprise of a mixture of the two isomers illustrated.

was attempted, this time from chloroform. In this case and possibly because of the lower anisometry of the complex, the best that could be obtained was a 10 : 1 mixture, but here it proved possible to obtain single crystals suitable for X-ray diffraction analysis. The molecular structure is shown as Fig. 3, accompanied by key structural parameters in Table 1. It should be noted that the chemical shifts of the methine hydrogens in these two isomers are identical to those in the di(alkoxyphenyl)pyridine complexes and that, in this case also, it is the isomer where this

Table 4 Isomer ratios obtained on preparation of complex **6**–6 in different solvents at different temperatures. All reactions were run overnight

Solvent	*T*/°C	Isomer ratio[a]
CH_2Cl_2	0	5 : 1
CH_2Cl_2	Ambient	3 : 1
CH_2Cl_2	40	1 : 1
$CHCl_3$	Ambient	6 : 1
Acetone	Ambient	No reaction

[a] Identified as the ratio of the complex giving rise to the signal at $\delta = 5.80$ and that at $\delta = 5.84$.

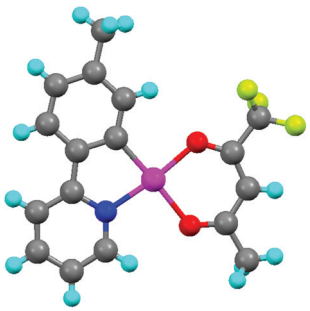

Fig. 3 Molecular structure of complex **12**. An ORTEP representation using thermal ellipsoids is found as Fig. S2(b).‡

hydrogen resonates at $\delta = 5.80$ that is concentrated.

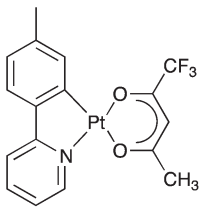

12

The structure was solved with one chloroform solvent molecule of crystallisation in the asymmetric unit, which was modelled isotropically as disordered over three positions in a 39.5 : 37 : 23.5 ratio. All C–Cl bond lengths were constrained to be similar and all Cl–C–Cl 1,3-bond distances were constrained to be similar. Several large peaks of residual electron density remained which could not be explained satisfactorily by disorder models and attempts to find a twin law were similarly unsuccessful. The two large peaks of residual density close to the platinum are believed to be due to non-merohedral twinning of the crystal, although a suitable method could not be obtained to account for this.

The asymmetric unit thus contains two complex molecules along with one (disordered) $CHCl_3$ of crystallisation (Fig. S2‡) and there were no statistically significant differences in the bond lengths between the two complexes in the unit cell (Table 2). The two Pt–O bonds were different in length reflecting the different *trans* influences of carbon and nitrogen, with the longer Pt–O bond being that *trans* to carbon as expected (Table 2). The

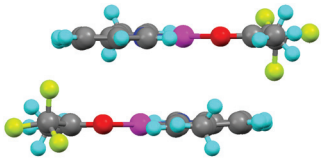

Fig. 4 Side-on view of the dimeric, face-to-face arrangement of the Pt complexes.

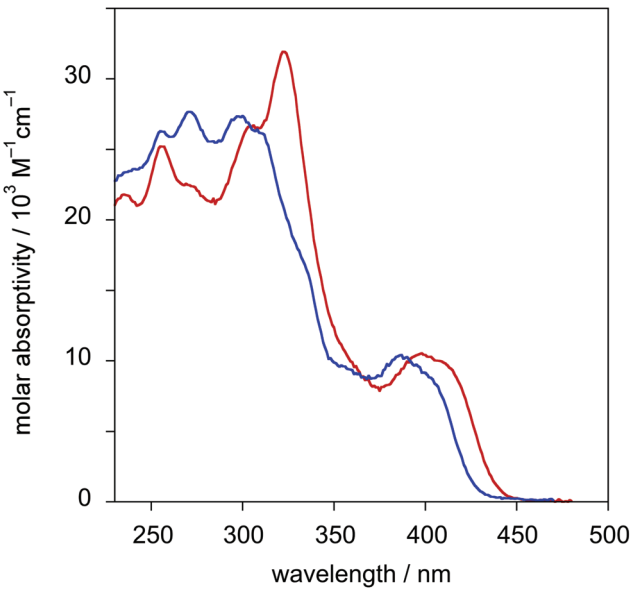

Fig. 5 UV-visible absorption spectra of the pair of complexes with heptanedionate as the co-ligand, with (blue) and without (red) the fused cyclopentane ring.

complexes arranged themselves as dimers through a formal centre of inversion (see Fig. 4 for a side-on view of the arrangement and Fig. S3‡ for a top view). The distance between the two planes defined by Pt and the two oxygens and three carbons of the tfac ligand framework is 3.39 Å, while the distance between the two, offset Pt atoms is 4.684 Å.

It is postulated, therefore, that the isomer that it is possible to isolate in the liquid-crystalline derivatives is also that found here, in which the CF_3 group is positioned *anti* with respect to the Pt–N bond. It is interesting that this is consistent with a qualitative proposal that this isomer is less polar owing to the anti disposition of the more polar Pt–N bond (wrt Pt–C) and the CF_3 group and so would be expected to crystallise preferentially from acetone (then later chloroform) as a polar solvent, which was the working hypothesis employed until the single crystal was obtained.§

Photophysics of the new complexes

The UV-visible absorption spectra of the complexes in solution display profiles that are typical of cyclometallated Pt^{II} complexes of arylpyridines[6] (*e.g.* Fig. 5 and Table 5). Intense absorption bands ($\varepsilon > 10\,000\ M^{-1}\ cm^{-1}$) in the region < 330 nm are due to π–π* transitions of the conjugated ligands, whilst the bands at longer wavelength tailing into the visible region have no counterparts in the free ligands and are associated with charge-transfer bands involving the combination of metal and ligand. These low-energy bands are blue-shifted in the complexes incorporating the fused cyclopentane ring compared to those without, which probably reflects the steric influence of the *ortho*-CH_2 groups of the cyclopentene ring which will serve to inhibit conjugation between the two rings.[9d] On the other hand, the identity of the *O^O* co-ligand is seen to have little influence on the absorption energies (Table 4).

All of the complexes incorporating heptanedionate or trifluoroacetylacetonate are strongly luminescent in degassed solution at room temperature, emitting in the green-yellow region of the visible spectrum (Fig. 6). The spectra are similar to those with acac as the co-ligand reported previously.[9d] They are red-shifted compared to that of [Py(ppy)(acac)], reflecting the expected influence of the electron-donating methoxy group in raising the HOMO level, which is typically localised primarily on the cyclometallating aryl unit and the metal, and the more extended conjugation arising from the aryl ring appended on the pyridyl unit. The higher energy of emission of the complexes incorporating the fused cyclopentane ring compared to those without (Fig. 6) mirrors the effect in absorption described above, due to the likely inhibition of attainment of a planar conformation that maximises conjugation in the ligand. Although the spectra display some evidence of vibrational structure, it is less pronounced than in [Pt(ppy)(acac)], perhaps reflecting the larger number of vibrational and rotational modes introduced with the additional aryl ring.

The quantum yields of luminescence are impressively high, in the range 0.5 to 0.7, amongst the highest reported for platinum(II) complexes with bidentate cyclometallating ligands.[6c] The luminescence lifetimes are around 25 μs, similar to those recorded previously for the acac complexes, and an order of magnitude longer than for [Pt(ppy)(acac)].[6c] Formerly, we interpreted this elongation of the lifetime in terms of a decrease in both the non-radiative and radiative rate constants.[9d] The former probably arises because of the delocalisation of the excited state over the pendent aryl ring at position 5 of the pyridyl ring, rendering it less well coupled to deactivating vibrational modes associated with the acac. The latter effect may reflect the decrease in metal character in the excited state with more extended delocalisation over the ligand, and hence less efficient spin–orbit coupling to promote the formally forbidden radiative decay of the triplet state.

Despite the existence of two isomeric complexes in the samples of the tfac complexes, there is no evidence of any additional bands in their emission spectra compared to those with the hdn co-ligand, nor do the spectra appear to be noticeably broader [compare spectra (b) with spectra (a) in Fig. 6]. This could indicate either that both isomers of the tfac complexes emit at essentially the same energy, or that one of the isomers is significantly more luminescent and dominates the spectrum.

We chose to try to probe this point in a little more detail using complex **6**–6, given that it had proved possible to isolate an almost pure sample of one isomer in this case, as described earlier. First, considering the sample of this complex comprising

§ Note that we did attempt to record a ^1H NMR spectrum of the single crystal used in the diffraction study. However, the crystal was obtained from an oily residue and the resulting spectrum could not be used with any certainty to draw useful conclusions.

Table 5 Absorption and emission data for the platinum(II) complexes in CH_2Cl_2 at 298 K

	Complexes *without* cyclopentane ring				Complexes with pyridyl-fused cyclopentane ring			
	7 hfac	**6**–12 tfac	**5**–12 hdn	**4**–12 acac	**11** hfac	**10** tfac	**9** hdn	**8**–12 acac
Absorption – λ_{max}/nm ($\varepsilon/10^3$ M^{-1} cm^{-1})	391 (15.7), 314 (32.5), 262 (24.2), 241 (20.8)	392 (13.2), 318 (34.5), 303 (25.2), 266 (24.9), 250 (24.0)	397 (10.5), 323 (31.8), 306 (26.4), 270 (22.7), 256 (23.1), 235 (21.2)	400 (8.2), 322 (30.5), 305 (24.7), 272 (18.3), 255 (20.4)	379 (15.4), 304 (28.2), 332 (12.9), 293 (26.3), 263 (28.9), 244 (23.5),	379 (13.3), 307 (28.1), 265 (29.8), 252 (27.5)	386 (10.4), 360 (9.3), 309 (28.6), 298 (27.5), 271 (27.6), 256 (26.0), 241 (22.9)	400 (8.9), 386 (10.3), 298 (28.2), 271 (27.1), 256 (25.0)
Emission – λ_{max}/nm	—	544, 581	545, 583	541, 582, 628 (sh)	—	525, 555	526, 554	523, 553, 608 (sh)
Lifetime – τ degassed (air equilibrated)/μs	—	26 (0.56)	30 (0.50)	27 (0.55)	—	23 (0.35)	26 (0.37)	27 (0.38)
Quantum yield – ϕ_{lum}	—	0.70	0.62	0.49	—	0.53	0.61	0.57

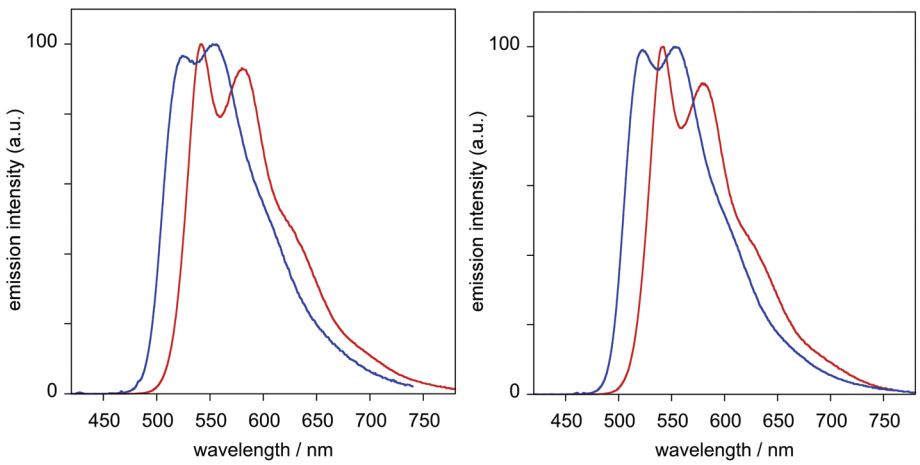

Fig. 6 (a) Left: Emission spectra of the pair of complexes with heptanedionate as the co-ligand, with (blue) and without (red) the fused cyclopentane ring, λ_{ex} = 400 nm. (b) Corresponding spectra for the complexes with trifluoroacetylacetonate as the co-ligand.

a 1 : 1 mixture of isomers, only one set of bands was observed in the emission spectrum at room temperature. However, for a sample in EPA glass (EPA = diethyl ether–isopentane–ethanol, 2 : 2 : 1 v/v) at 77 K, the emission spectrum revealed a clear additional shoulder to high energy of the main bands (Fig. 7). Moreover, when the sample comprising one isomer concentrated to 36 : 1 was examined under the same conditions, the spectrum was clearly shifted to high energy, with the position of the 0–0 band matching well with the higher-energy shoulder observed in the 1 : 1 sample (Fig. 7). Thus, we tentatively conclude that the isomer that had been concentrated (*viz.* that with the CF_3 trans to Pt–N) emits at higher energy than the other, and with a significantly lower quantum yield, such that, in the 1 : 1 samples, it is the emission of the other isomer that dominates the spectrum.

In contrast to the complexes incorporating hdn and tfac co-ligands, those containing hexafluoroacetyl acetonate showed no luminescence at room temperature. The absence of emission from these complexes is at first sight surprising, given that the excited state in [Pt(*N^C*)(*O^O*)] complexes is normally based largely on the metal and the cyclometallating ligand, with the β-diketonate acting essentially as an 'innocent' auxiliary ligand. Time-dependent density functional theory provides insight into the origin of the difference between the hfac and the tfac/acac complexes.

Density functional theory calculations

In order to probe the influence of the co-ligand (*i.e.* acac, tfac or hfac) on the emissive excited state in the three types of complex, and also the influence of the isomerism in the tfac systems, time-dependent density functional theory has been applied. To simplify the calculations, the four representative unsubstituted complexes shown in Fig. 8 were considered. The two tfac isomers are labeled *cis* and *trans*, on the basis of the relative disposition of the CF_3 and pyridyl groups.

Calculations were carried out with the LANL2DZ basis set for Pt^{II} and cc-PVDZ basis set for the ligands, using both PBE0 and CAM-B3LYP functionals. The use of Coulomb-attenuated functionals, of which CAM-B3LYP is a well-established example,[12] is frequently superior to more conventional functionals when excited states with significant charge-transfer character are under investigation.[13,14] The calculations were applied to the gas-phase molecules and also in dichloromethane (using the polarisable continuum model) to check for any significant solvent effect.

The ground-state geometries were first optimised without symmetry constraints, and harmonic frequency calculations performed to confirm the attainment of energy minima on the potential energy surface. The key bond lengths and angles involving the metal, predicted by DFT in this way for *cis* and *trans*-[Pt(ppy)(tfac)] in the ground state, are illustrated in Fig. 9. There is good agreement between the calculated data and the experimentally determined bond lengths in the crystal of complex **12** listed in Table 2. However, it may be noted that there are no significant differences between the two isomers.

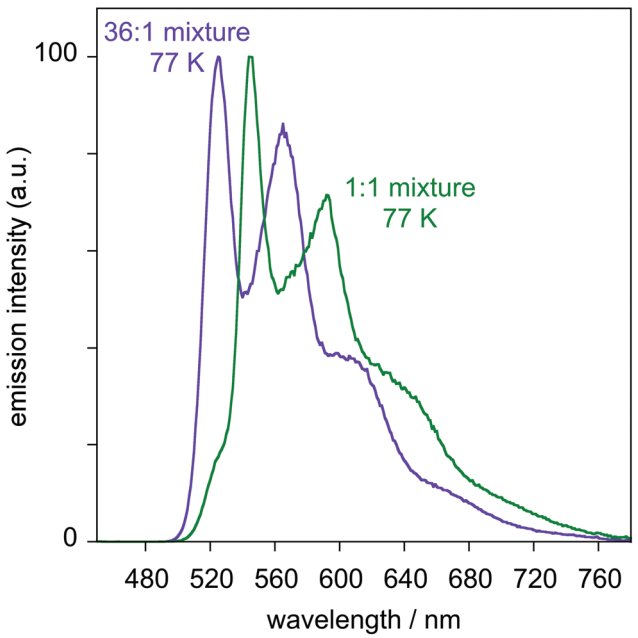

Fig. 7 The emission spectra of **6**–6 in diethyl ether–isopentane–ethanol (2 : 2 : 1 v/v) at 77 K. Green line: the spectrum of the 1 : 1 mixture of isomers. Purple line: corresponding spectrum of the sample in which one isomer has been concentrated to 36 : 1 by fractional recrystallisation.

Plots of the frontier orbitals (HOMO − 2 to LUMO + 2) obtained by TD-DFT are shown in the ESI (Fig. S4–S7‡) with energies of orbitals listed in Table S1.‡ Similar results were obtained using CAM-B3LYP as for PBE0, probably due to a reasonably high degree of orbital overlap despite the element of charge-transfer character to the excited state.[14] Since the lowest-energy triplet excited states comprise varying proportions of excitations involving different orbitals, and are not exclusively HOMO → LUMO in character, it is more appropriate and informative to inspect the density difference plots, which display the net rearrangement of the electron density in the excited state compared to the ground state. The density difference plots of the lowest triplet excitation – most relevant to the emission – are shown in Fig. 10. They reveal that the two [Pt(ppy)(tfac)] isomers feature excited states that are similar to that of [Pt(ppy)-(acac)]. There is depletion of electron density on the metal and cyclometallating aryl ring, with an increase on the pyridyl ring, consistent with the usual formulation of the excited states in such complexes as $d_{Pt}/\pi_{N^{\wedge}C} \rightarrow \pi^*_{N^{\wedge}C}$ (mixed MLCT/LLCT). In contrast, the triplet excited state of [Pt(ppy)(hfac)] has very different character: it involves the movement of the electron from the metal and aryl ring of the ppy to the hfac co-ligand. Apparently, this arises because the presence of the two electron-withdrawing CF_3 groups stabilises the π* orbitals associated with the co-ligand to such an extent that the LUMO becomes based on the hfac rather than on the ppy (Fig. S4–S7‡). Indeed, the LUMO for [Pt(ppy)(hfac)] is seen to be similar to LUMO + 2 for the acac complex. Quite similar conclusions were drawn by Ghedini *et al.* on related cyclometallated Pt^{II} and Pd^{II} complexes with hfac co-ligands, where an inversion of the ordering of LUMO and LUMO + 1 was observed on changing from acac to hfac.[15]

The lack of emission from the hfac complexes might then be attributable – at least in part – to the poor overlap of the orbitals involved in the excitation, the orbitals being localised on different parts of the molecule, leading to a low radiative rate constant. Absence of emission has likewise been observed and rationalised

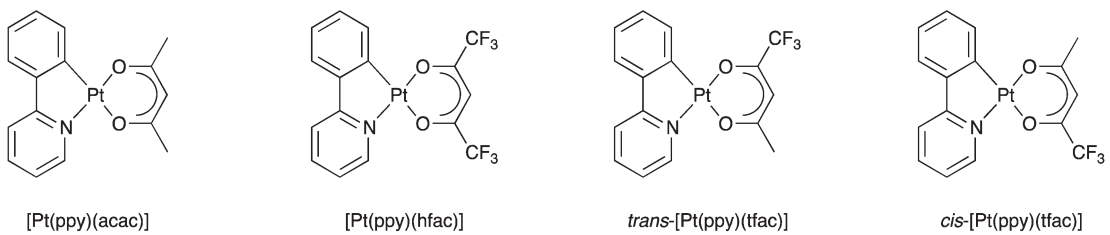

Fig. 8 Structures of the four complexes studied by TD-DFT.

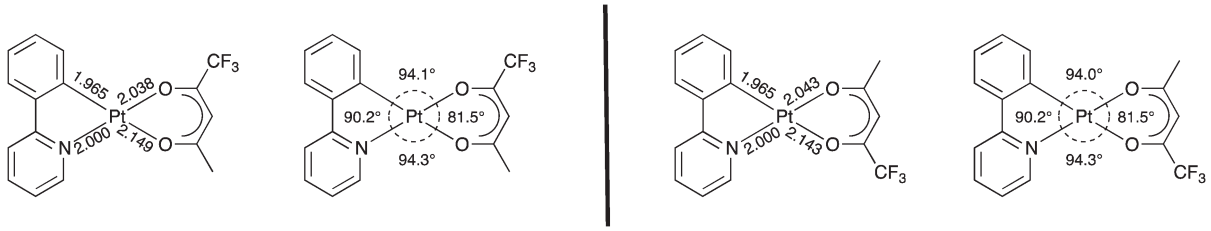

Fig. 9 Bond lengths (Å) and angles (°) determined by TD-DFT for the ground state of the *trans*- (left) and *cis*- (right) isomers of [Pt(ppy)(tfac)].

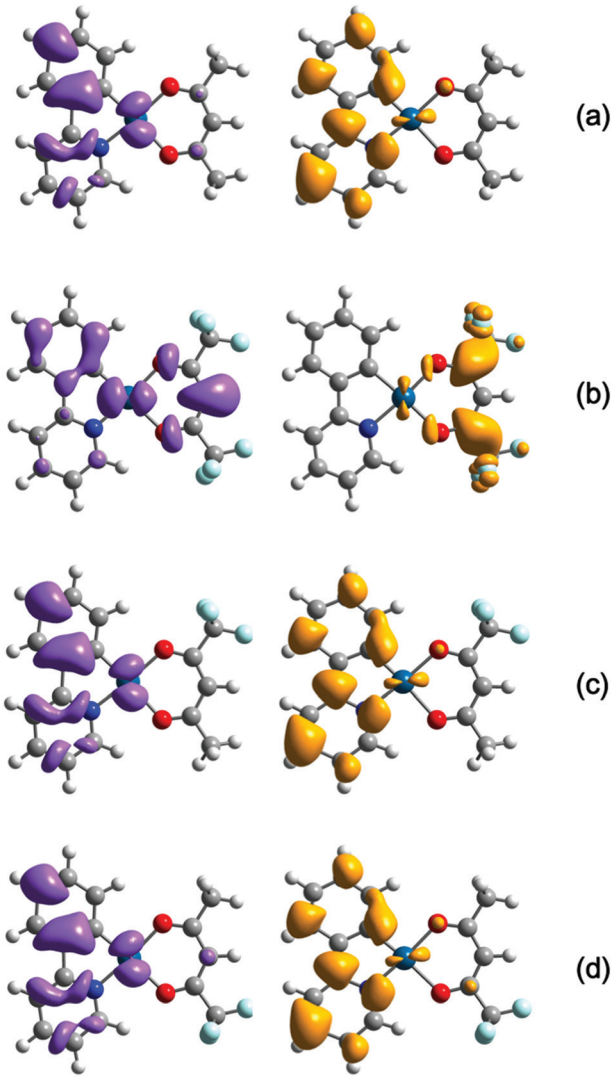

Fig. 10 Density difference plots for the lowest triplet excitations of the four complexes at the ground-state geometry: (a) [Pt(ppy)(acac)], (b) [Pt(ppy)(hfac)], (c) *trans*-[Pt(ppy)(tfac)], (d) *cis*-[Pt(ppy)(tfac)]. Purple and yellow represent zones of depletion and augmentation of electron density, respectively. Calculated using PBE0 with the PCM model for CH_2Cl_2 as solvent.

in the same way for cyclometallated iridium(III) complexes in which the frontier orbitals are localised on different ligands, with little overlap.[16] However, substantial distortion in the triplet excited state of the hfac complexes may also play a role in disfavouring emission (*vide infra*).

Although the calculations help to understand the different behaviour of the hfac complexes, there is little difference between the density difference plots of the two isomers of [Pt(ppy)(tfac)], even though the experimental data suggest that one form is significantly more emissive than the other, as discussed earlier. The energies of the orbitals calculated for the two isomers are very similar to one another (Table S1‡). It is notable, however, that the presence of one CF_3 group leads to LUMO + 1 being the orbital most similar to LUMO in the hfac complex, but to LUMO + 2 in the acac complex (Fig. S4–S7‡). In other words, the unoccupied orbital based on the *O^O* co-ligand is clearly

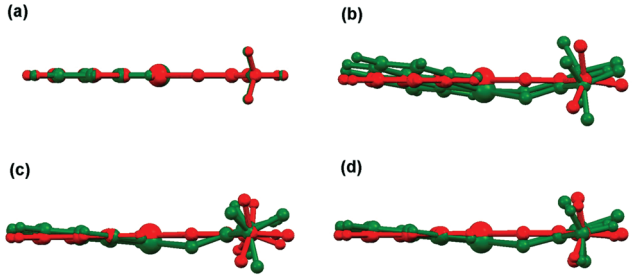

Fig. 11 Superimposed structures of the S_0 ground state (red) and T_1 excited state (green) for the four complexes of Fig. 8, optimised using PBE0 with the polarisable continuum model for CH_2Cl_2. (a) [Pt(ppy)(acac)]; (b) [Pt(ppy)(hfac)]; (c) *trans*-[Pt(ppy)(tfac)]; (d) *cis*-[Pt(ppy)(tfac)].

stabilised in the tfac complexes relative to the acac, but not sufficiently so to make it the LUMO, as occurs in the case of the hfac complex.

Triplet state geometries

Although it is commonplace to assume, in calculations of this sort, that the triplet state of metal complexes will have the same geometry as the ground state, there is clearly no reason why this should necessarily be the case. For the purpose of understanding the emission properties, it should, therefore, be useful to consider the extent to which the structure of the molecule in its triplet state is distorted compared to the ground state, since large distortions typically promote non-radiative decay with a correspondingly detrimental effect on quantum yields. The triplet-state geometries of the two isomers were therefore calculated by direct minimisation of the SCF triplet state, again using the polarisable continuum model for the dichloromethane solvent.

The triplet-state structures obtained in this way are shown in Fig. 11. Strikingly, it can be seen that [Pt(ppy)(acac)] remains essentially planar in the excited state, whereas the tfac and hfac complexes show some distortion. The distortion is quite clearly largest for [Pt(ppy)(hfac)]. This feature could help account for the lack of emission observed for the hfac complexes: greater distortion in the excited state would increase non-radiative decay, compounding the lower radiative rate constant predicted on the basis of the poorer frontier orbital overlap discussed above.

Moreover, the analysis may provide insight into the origin of the difference in emission efficiencies of the two isomers of [Pt(ppy)(tfac)]. If the extent of distortion is quantified in terms of the root-mean-square displacement of the atoms between the S_0 and T_1 structures, or indeed the maximum displacement of any atom (Table 6), the degree of distortion can be seen to increase in the order [Pt(ppy)(acac)] < *cis*-[Pt(ppy)(tfac)] < *trans*-[Pt(ppy)(tfac)] < [Pt(ppy)(hfac)]. The weaker emission tentatively attributed to the *trans* compared to the *cis* isomer of [Pt(ppy)(tfac)] might thus be accounted for in terms of the greater triplet excited state distortion in the former, leading to enhanced non-radiative decay.

Cyclic voltammetry and EPR spectroscopy

Interested by the observation that the hfac complexes studied (**7** and **11**) were not emissive and the possible explanation in

terms of the differing localisation of the LUMO, a comparative study was made of the cyclic voltammograms of representative hfac and tfac complexes.

Complexes of the Pt(*N^C*)(*O^O*) type that are emissive are typically characterised by a chemically irreversible reduction on population of the LUMO, which is mainly based on the 2-phenylpyridine unit.[8] This is indeed the case here and the cyclic voltammogram (Fig. 12) of **6**–12 shows the reduction wave with $E_{peak} \approx -1.0$ V (relative to the Fc/Fc^{+} couple at 0.64 V). However, when the hfac complex **7** was studied, the reduction process was found to be *reversible* (Fig. 12).

Keen to explore further the nature of the species formed on reduction of **7**, the reduction was then performed in an epr cavity and the spectrum shown in Fig. 13 was obtained. The spectrum was simulated assuming a binomial septet (a_F = 2.16 mT) due to coupling to the six equivalent fluorines, which is further split into a doublet (a_H = 0.23 mT) due to coupling to the methine hydrogen. In addition, there are platinum satellites (a^{195}_{Pt} = 2.43 mT). The spectrum shows considerable anisotropy, which manifests itself as a significant increase in the linewidth with increasing magnetic field. The spectrum was simulated using Easyspin[17] by allowing the linewidths to vary with the major septet component from low field to high field as follows (1–0.07 mT, 6–0.08 mT, 15–0.09 mT, 20–0.12 mT, 15–0.17 mT, 6–0.24 mT, 1–0.35 mT). Whilst this is a simplification of the anisotropic processes, it does confirm that the splitting parameters reported are consistent with the experimental spectrum observed. The spectrum is consistent with the radical character being that of the radical di-anion of hfac with an additional coupling to the platinum, and the splittings are similar to those observed for the alkali metal and tetraalkylammonium salts of the free radical di-anion.[18]

This simulation therefore requires that the electron be localised on the hfac ligand. This conclusion is fully consistent with the

Table 6 Root-mean-square displacement of atoms and maximum displacement of any atom on going from the S_0 to T_1 structures of the complexes, as determined from the optimised geometries obtained by TD-DFT using PBE0 and PCM for CH_2Cl_2 solvent

Compound	Root-mean-square displacement/Å	Maximum displacement/Å
[Pt(ppy)(acac)]	0.0261	0.0531
[Pt(ppy)(hfac)]	0.4185	0.8176
trans-[Pt(ppy)(tfac)]	0.3101	0.7382
cis-[Pt(ppy)(tfac)]	0.2496	0.6478

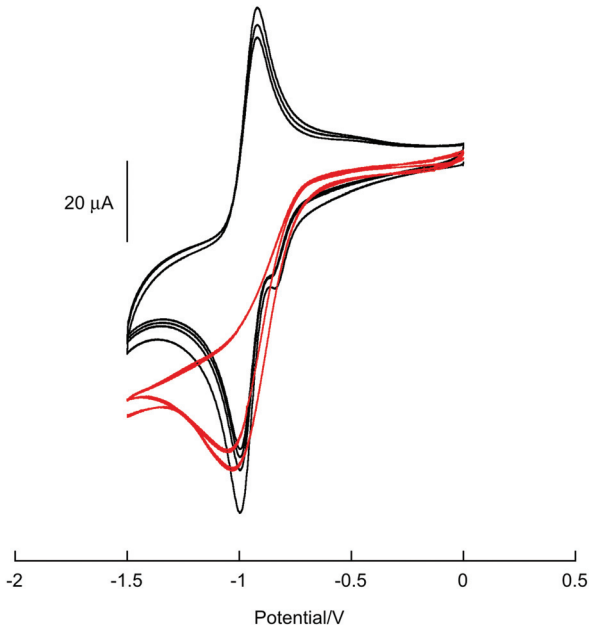

Fig. 12 Cyclic voltammogram of complex **6**–12 (red lines), showing an irreversible reduction, and of complex **7** (black lines) showing a reversible reduction. Scan rate was 100 mV s^{-1} and the reference electrode was Ag/AgCl; $[FeCp_2]^{0/+}$ is found at 0.64 V in this cell.

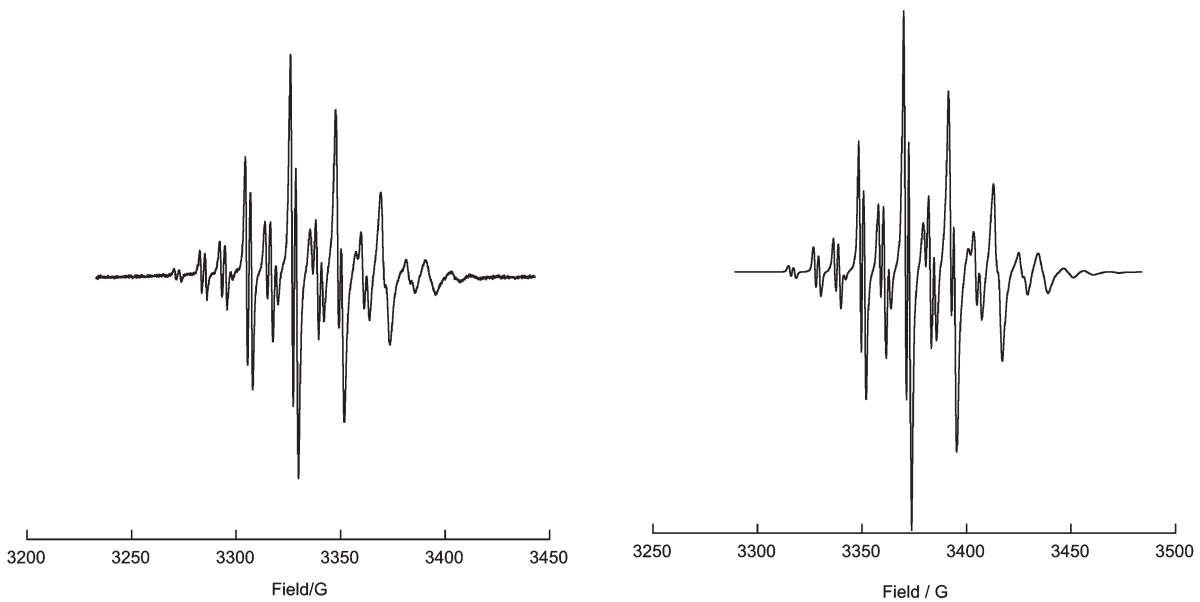

Fig. 13 Real (left) and simulated (right) EPR spectra of the monoanion of **7**. Simulation parameters are given in the text. The superimposed spectrum and simulation are given as Fig. S8.‡ Spectrum was recorded at 25 °C.

results of the TD-DFT calculations discussed in the previous section, where the LUMO for the hfac complex was found to be localised on the hfac ligand (*e.g.* Fig. S5b‡). This contrasts with the results for the tfac complexes, for which the LUMO was found to be similar to that of the acac complex, being located primarily on the ppy ligand (*e.g.* Fig. S5a, c and d‡).

Experimental

^{1}H NMR spectra were recorded at 270 MHz using a JEOL ECX270 instrument, while optical microscopy employed an Olympus BX50 Optical Microscope equipped with a Link-Am HFS91 hot stage, TMS92 controller and LNP2 cooling unit. DSC data were collected using a Mettler Toledo DSC 822, equipped with a TSO801R0 sample robot and calibrated using indium; samples were run at heating and cooling rates of 10 °C min^{-1}. Elemental analysis was carried out on an Exeter Analytical Inc CE 440 Elemental Analyser and a Sartorius SE2 analytical balance at the University of York.

X-band EPR data were recorded at 25 °C on an Bruker ER 200-D SRC X-band spectrometer connected to a datalink 486DX desktop PC running EPR Acquisition System version 2.42. A specially designed[19] variable-temperature, *in situ* cell was used with a platinum gauze working electrode placed in the flat part of the cell. Platinum wire counter and Ag/AgCl reference electrodes were placed on the reservoir at the top of the cell. Electrogeneration was performed using a Potentiostat BASCV-27 Voltammograph. All *g*-values were referenced to the *g*-value of 2,2′-diphenyl-1-picrylhydrazyl (DPPH) at 2.0036 ± 0.002.[20]

Diffraction data were collected at 110 K on a Bruker Smart Apex diffractometer with Mo-K_α radiation (λ = 0.71073 Å) using a SMART CCD camera. Diffractometer control, data collection and initial unit cell determination was performed using 'SMART'.[21] The crystal was cooled with an Oxford Cryostream. Frame integration and unit-cell refinement was carried out with 'SAINT+'.[22] Absorption corrections were applied by SADABS.[23] Structures were solved by 'direct methods' using SHELXS-97 (Sheldrick, 1997)[24] and refined by full-matrix least squares using SHELXL-97 (Sheldrick, 1997).[25] All non-hydrogen atoms were refined anisotropically, whereas the disordered chloroform was refined isotropically. O–H hydrogens were located by difference map after all other atoms had been located and refined. All other hydrogen atoms were placed using a 'riding model' and included in the refinement at calculated positions.

A Voltalab 50, PST050, produced by Radiometer Analytical was used to record cyclic voltammograms. The reference electrode was Ag/AgCl and the working electrode was platinum. The voltammograms were recorded at 50 and 100 mV s^{-1} in DMF containing $[Bu_4N][PF_6]$ (0.1 mol dm^{-3}) using $[FeCp_2]^{0/+}$ at 0.64 V as internal standard.

Photophysical measurements

Absorption spectra were measured on a Biotek Instruments XS spectrometer, using quartz cuvettes of 1 cm pathlength. Steady-state luminescence spectra were measured using a Jobin Yvon FluoroMax-2 spectrofluorimeter, fitted with a red-sensitive Hamamatsu R928 photomultiplier tube; the spectra shown are corrected for the wavelength dependence of the detector, and the quoted emission maxima refer to the values after correction. Samples for emission measurements were contained within quartz cuvettes of 1 cm pathlength modified with appropriate glassware to allow connection to a high-vacuum line. Degassing was achieved *via* a minimum of three freeze–pump–thaw cycles whilst connected to the vacuum manifold; final vapour pressure at 77 K was $<10^{-2}$ mbar, as monitored using a Pirani gauge. Luminescence quantum yields were determined using $[Ru(bpy)_3]Cl_2$ in aqueous solution (Φ = 0.028)[26] as the standard; estimated uncertainty in Φ is ±20% or better.

The luminescence lifetimes of the complexes in aerated solution were measured by time-correlated single-photon counting (TCSPC), following excitation at 374.0 nm with an EPL-375 pulsed diode laser. The emitted light was detected at 90° using a Peltier-cooled R928 PMT after passage through a monochromator. The lifetimes in degassed solution were determined by multichannel scaling using the same detector following excitation with a pulsed xenon lamp.

TD-DFT calculations

DFT calculations were carried out using the Gaussian 09[27] suite of programmes to predict energy-minimized structures of both the singlet ground state and lowest triplet excited state of the complexes. The LANL2DZ basis set was used for Pt^{II}, with the inner core electrons replaced by a relativistic core potential; the all-electron cc-PVDZ basis set for the ligands. Calculations were carried out using two different functionals, PBE0[28] and CAM-B3LYP,[12] in both the gas phase and with the polarizable continuum model (pcm) solvent model for dichloromethane (as specified) using the default Gaussian 09 cavity parameters. Geometries were fully optimized without symmetry constraints. The triplet-state structures were calculated by direct minimisation of the SCF triplet state. Harmonic vibrational wavenumber calculations were performed to confirm that the structures obtained correspond to minima of the potential energy surface. Time-dependent calculations were carried out on the optimised structures to investigate the relevant transitions and for the generation of density difference plots.

Synthesis

Ligands and complexes were prepared as described in ref. 9*d*, as outlined in Scheme 1. The final step was reaction of [Pt(*N^C*)-Cl(*S*-dmso)] with the sodium salt of the β-diketonate and conditions did not depend on the diketone used. Preparations of these sodium salts is given below. Analytical data for the new complexes are found in the ESI as Table S2.‡

Synthesis of sodium hexafluoroacetylacetonate

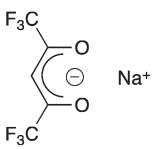

Hexafluoroacetylacetone (14.4 mmol, 3.00 g) was added to sodium ethoxide (14.4 mmol, 0.98 g) in petroleum ether

(50 cm^3). The mixture was heated under reflux for 4 h. After cooling to room temperature, the colourless precipitate was recovered by filtration and washed with petroleum ether (10 cm^3). Yield: 1.83 g, 55.3%.

Synthesis of sodium trifluorofluoroacetylacetonate

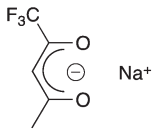

1,1,1-Trifluoro-2,4-pentanedione (3.24 mmol, 0.50 g) was added to sodium hydride (3.24 mmol, 77.8 mg) in petroleum ether (15 cm^3), the solution was heated under reflux for 1 h. After cooling to room temperature, the colourless precipitate was recovered by filtration and washed with petroleum ether (10 cm^3). Yield: 0.54 g, 94.5%.

Synthesis of sodium 3,5 heptanedionate

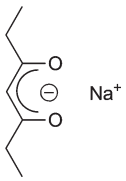

3,5-Heptanedione (3.90 mmol, 0.50 g) was added to sodium hydride (3.90 mmol, 93.6 mg) in petroleum ether (15 cm^3), the solution was stirred at room temperature 1 h. The colourless precipitate was recovered by filtration and washed with petroleum ether (10 cm^3). Yield: 0.48 g, 82.5%.

Acknowledgements

We thank EPSRC (AD, GRF), the University of York (AS), the University of Edinburgh (PRM) and the Comunidad Autonoma de la Rioja (JT) for funding, Johnson Matthey for generous loans of $K_2[PtCl_4]$ and Dr Victor Chechik (University of York) for valuable discussions concerning the epr spectrum.

References

1 (*a*) S. Laschat, A. Baro, N. Steinke, F. Giesselmann, C. Hägele, G. Scalia, R. Judele, E. Kapatsina, S. Sauer, A. Schreivogel and M. Tosoni, *Angew. Chem., Int. Ed.*, 2007, **46**, 4832; (*b*) S. Xiao, M. Myers, Q. Miao, S. Sanaur, K. Pang, M. L. Steigerwald and C. Nuckolls, *Angew. Chem., Int. Ed.*, 2005, **44**, 7390; (*c*) J. Nelson, *Science*, 2001, **293**, 1059; (*d*) L. Schmidt-Mende, A. Fechtenkötter, K. Müllen, E. Moons, R. H. Friend and J. D. Mackenzie, *Science*, 2001, **293**, 1119; (*e*) S. R. Forrest, *Nature*, 2004, **428**, 911.
2 M. O'Neill and S. M. Kelly, *Adv. Mater.*, 2011, **23**, 566; M. O'Neill and S. M. Kelly, *Adv. Mater.*, 2003, **15**, 1135.
3 Y. Sagara and T. Kato, *Angew. Chem., Int. Ed.*, 2008, **47**, 5175.
4 V. N. Kozhevnikov, B. Donnio and D. W. Bruce, *Angew. Chem., Int. Ed.*, 2008, **47**, 6286.
5 (*a*) A. M. Prokhorov, A. Santoro, J. A. G. Williams and D. W. Bruce, *Angew. Chem., Int. Ed.*, 2012, **51**, 95; (*b*) A. Santoro, A. M. Prokhorov, A. C. Whitwood, B. Donnio, J. A. G. Williams and D. W. Bruce, *J. Am. Chem. Soc.*, 2011, **133**, 5248; (*c*) Y. Wang, Q. Chen, Y. Li, Y. Liu, H. Tan, J. Yu, M. Zhu, H. Wu, W. Zhu and Y. Cao, *J. Phys. Chem. C*, 2012, **116**, 5908; (*d*) E. L. Szerb, A. M. Talarico, I. Aiello, A. Crispini, N. Godbert, D. Pucci, T. Pugliese and M. Ghedini, *Eur. J. Inorg. Chem.*, 2010, **21**, 3270–3274; (*e*) K. Binnemans, in *Molecular Materials*, ed. D. W. Bruce, D. O'Hare and R. I. Walton, Wiley, Chichester, 2010, pp. 61–141; (*f*) K. Binnemans, *J. Mater. Chem.*, 2009, **19**, 448; (*g*) D. Pucci, *Liq. Cryst.*, 2011, **38**, 1451; (*h*) E. Terazzi, S. Suarez, S. Torelli, H. Nozary, D. Imbert, O. Mamula, J. P. Rivera, E. Guillet, J. M. Benech, G. Bernardinelli, R. Scopelliti, B. Donnio, D. Guillon, J.-C. G. Bünzli and C. Piguet, *Adv. Funct. Mater.*, 2006, **16**, 157; (*i*) Y. T. Yang, K. Driesen, P. Nockermann, K. Van Hecke, L. Van Meervelt and K. Binnemans, *Chem. Mater.*, 2006, **18**, 3698; (*j*) Y. Galyametdinov, A. A. Knyazev, V. I. Dzhabarov, T. Cardinaels, K. Driesen, C. Görller-Walrand and K. Binnemans, *Adv. Mater.*, 2008, **20**, 252; (*k*) R. Bayón, S. Coco and P. Espinet, *Chem.–Eur. J.*, 2005, **11**, 1079.
6 (*a*) W. Paw, S. D. Cummings, M. A. Mansour, W. B. Connick, D. K. Geiger and R. Eisenberg, *Coord. Chem.Rev.*, 1998, **171**, 125; (*b*) M. Hissler, J. E. McGarrah, W. B. Connick, D. K. Geiger, S. D. Cummings and R. Eisenberg, *Coord. Chem. Rev.*, 2000, **208**, 115; (*c*) J. A. G. Williams, *Top. Curr. Chem.*, 2007, **281**, 205; (*d*) J. Reedijk, *Eur. J. Inorg. Chem.*, 2009, **10**, 1303; (*e*) M. D. Perez, P. I. Djurovich, A. Hassan, G. Y. Chang, T. J. Stewart, K. Aznavour, R. Bau and M. E. Thompson, *Chem. Commun.*, 2009, 4215; (*f*) W.-Y. Wong and C.-L. Ho, *Coord. Chem. Rev.*, 2008, **252**, 2596; (*g*) Z. M. Hudson, C. Sun, M. G. Helander, H. Amarne, Z. Lu and S. Wang, *Adv. Funct. Mater.*, 2010, **20**, 3426; (*h*) D. N. Kozhevnikov, V. N. Kozhevnikov, M. Z. Shafikov, A. M. Prokhorov, D. W. Bruce and J. A. G. Williams, *Inorg. Chem.*, 2011, **50**, 3804; (*i*) Z. M. Hudson, M. G. Helander, L. Zu and S. Wang, *Chem. Commun.*, 2011, **47**, 755; (*j*) Z. M. Hudson, B. A. Blight and S. Wang, *Org. Lett.*, 2012, **14**, 1700; D. A. K. Vezzu, J. C. Deaton, J. S. Jones, L. Bartolotti, C. F. Harris, A. P. Marchetti, M. Kondakova, R. D. Pike and S. Huo, *Inorg. Chem.*, 2010, **49**, 5107.
7 (*a*) W. Lu, B.-X. Mi, M. C.-W. Chan, Z. Hui, C.-M. Che, N. Zhu and S.-T. Lee, *J. Am. Chem. Soc.*, 2004, **126**, 4958; (*b*) S. Develay, O. Blackburn, A. L. Thompson and J. A. G. Williams, *Inorg. Chem.*, 2008, **47**, 11129; (*c*) L. Murphy and J. A. G. Williams, *Top. Organomet. Chem.*, 2010, **28**, 75; (*d*) J. Kalinowski, V. Fattori, M. Cocchi and J. A. G. Williams, *Coord. Chem. Rev.*, 2011, **255**, 2401; (*e*) A. Y.-Y. Tam, D. P.-K. Tsang, M.-Y. Chan, N. Zhu and V. W.-W. Yam, *Chem. Commun.*, 2011, **47**, 3383; (*f*) C. A. Strassert, C.-H. Chien, M. D. Galvez Lopez, D. Kourkoulos, D. Hertel, K. Meerholz and L. De Cola, *Angew. Chem., Int. Ed.*, 2011, **50**, 946; (*g*) E. Rossi, A. Colombo, C. Dragonetti, D. Roberto, F. Demartin, M. Cocchi, P. Brulatti, V. Fattori and J. A. G. Williams, *Chem. Commun.*, 2012, **48**, 3182.
8 J. Brooks, Y. Babayan, S. Lamansky, P. I. Djurovich, I. Tsyba, R. Bau and M. E. Thompson, *Inorg. Chem.*, 2002, **41**, 3055.
9 (*a*) K. Venkatesan, P. H. J. Kouwer, S. Yagi, P. Müller and T. M. Swager, *J. Mater. Chem.*, 2008, **18**, 400; (*b*) S. W. Thomas, S. Yagi and T. M. Swager, *J. Mater. Chem.*, 2005, **15**, 2829; (*c*) C. Damm, G. Israel, T. Hegmann and C. Tschierske, *J. Mater. Chem.*, 2006, **16**, 1808; (*d*) A. Santoro, A. C. Whitwood, J. A. G. Williams, V. N. Kozhevnikov and D. W. Bruce, *Chem. Mater.*, 2009, **21**, 3871.
10 A. Santoro, M. Wegrzyn, A. C. Whitwood, B. Donnio and D. W. Bruce, *J. Am. Chem. Soc.*, 2010, **132**, 10689.
11 L. Omnès, B. A. Timimi, T. Gelbrich, M. B. Hursthouse, G. R. Luckhurst and D. W. Bruce, *Chem. Commun.*, 2001, 2248.
12 T. Yanai, D. P. Tew and N. C. Handy, *Chem. Phys. Lett.*, 2004, **393**, 51.
13 M. J. G. Peach, P. Benfield, T. Helgaker and D. J. Tozer, *J. Chem. Phys.*, 2008, **128**, 044118.
14 P. Wiggins, J. A. G. Williams and D. J. Tozer, *J. Chem. Phys.*, 2009, **131**, 091101.
15 M. Ghedini, T. Puglise, M. La Deda, N. Godbert, I. Aiello, M. Amati, S. Belviso, F. Leji, G. Accorsi and F. Barigeletti, *Dalton Trans.*, 2008, **32**, 4303.
16 A. J. Wilkinson, H. Puschmann, J. A. K. Howard, C. E. Foster and J. A. G. Williams, *Inorg. Chem.*, 2006, **45**, 8685.
17 S. Stoll and A. Schweiger, *J. Magn. Reson.*, 2006, **178**, 142 (http://www.easyspin.org).
18 K. S. Chen and J. K. S. Wan, *J. Chem. Soc., Perkin Trans. 2*, 1982, 419.
19 P. Murray and L. Yellowlees, in *Spectroelectrochemistry*, ed. W. Kaim and A. Klein, Royal Society of Chemistry, Cambridge, 2008.
20 S. A. Al'tshuler and B. M. Kozyrev, *Electron Paramagnetic Resonance*, Academic Press, New York, 1964.
21 *'SMART' – Control Software Bruker SMART Apex X-ray Diffractometer. v5.625*, Bruker-AXS GMBH, Karlsruhe, Germany.
22 *'SAINT+' – integration software for Bruker SMART detectors. v6.45*, Bruker-AXS GMBH, Karlsruhe, Germany.

23 G. M. Sheldrick, *'SADABS' – Program for Absorption Correction. v2.10* Bruker AXS Inc., Madison, Wisconsin, USA, 2007.
24 G. M. Sheldrick, *SHELXS-97' – Program for Structure Solution* University of Göttingen, Göttingen, Germany, 1997.
25 G. M. Sheldrick, *SHELXL-97' – Program for the Refinement of Crystal Structures*, University of Göttingen, Göttingen, Germany, 1997.
26 K. Nakamaru, *Bull. Chem. Soc. Jpn.*, 1982, **55**, 2697.
27 M. J. Frisch, G. W. Trucks, H. B. Schlegel, G. E. Scuseria, M. A. Robb, J. R. Cheeseman, G. Scalmani, V. Barone, B. Mennucci, G. A. Petersson, H. Nakatsuji, M. Caricato, X. Li, H. P. Hratchian, A. F. Izmaylov, J. Bloino, G. Zheng, J. L. Sonnenberg, M. Hada, M. Ehara, K. Toyota, R. Fukuda, J. Hasegawa, M. Ishida, T. Nakajima, Y. Honda, O. Kitao, H. Nakai, T. Vreven, J. A. Montgomery, Jr., J. E. Peralta, F. Ogliaro, M. Bearpark, J. J. Heyd, E. Brothers, K. N. Kudin, V. N. Staroverov, R. Kobayashi, J. Normand, K. Raghavachari, A. Rendell, J. C. Burant, S. S. Iyengar, J. Tomasi, M. Cossi, N. Rega, J. M. Millam, M. Klene, J. E. Knox, J. B. Cross, V. Bakken, C. Adamo, J. Jaramillo, R. Gomperts, R. E. Stratmann, O. Yazyev, A. J. Austin, R. Cammi, C. Pomelli, J. W. Ochterski, R. L. Martin, K. Morokuma, V. G. Zakrzewski, G. A. Voth, P. Salvador, J. J. Dannenberg, S. Dapprich, A. D. Daniels, Ö. Farkas, J. B. Foresman, J. V. Ortiz, J. Cioslowski and D. J. Fox, *GAUSSIAN 09*, 2009.
28 J. P. Perdew, K. Burke and M. Ernzerhof, *Phys. Rev. Lett.*, 1996, **77**, 3865.

